

RESEARCH ARTICLE

Specific Emitter Identification of Frequency Hopping Signals Based on Feature Extraction and Deep Residual Network

MINGDI LI¹, JUN XIE^{1,2}, HONGJIE YANG¹, MENGJIE GENG^{1,2},
AND JICHUAN LIU^{1,2}, (Member, IEEE)

¹Signal Intelligence and Electronic Warfare Department, The 54th Research Institute of China Electronics Technology Group Corporation, Shijiazhuang, Hebei 050011, China

²Hebei Key Laboratory of Electromagnetic Spectrum Cognition and Control, Shijiazhuang, Hebei 050011, China

Corresponding author: Mingdi Li (937456214@qq.com)

This work was supported by the National Natural Science Foundation of China under Grant U20B2071.


ABSTRACT In the modern war with complex and changeable electromagnetic environment, Specific Emitter Identification (SEI) is an important and difficult problem, which is of great significance in obtaining intelligence information, identifying ourselves or foe, and specifying combat plans. In order to solve the problems of low accuracy, poor robustness and difficulty in extracting effective individual features of frequency hopping (FH) radio set, this paper studies the generation of PSK signal constellation to propose a radio frequency fingerprint (RFF) based on constellation. We also improved the existing RFF extraction method, combined with the deep learning recognition method based on the Deep Residual Network (ResNet), to achieve effective feature fusion. By comparing different input methods, we found that the recognition accuracy is improved, and reaches 96.16% in the outfield experiments of 15 FH radio sets. In addition, we also designed a ResNet structure to compare the recognition accuracy under different signal-to-noise ratio (SNR), different network structure, different number of individuals, different modulation methods and different recognition algorithms, which proved the superiority of our method.

INDEX TERMS Specific emitter identification (SEI), frequency hopping (FH) signal, constellation fingerprint features, deep residual network (ResNet), feature fusion.

I. INTRODUCTION

With the development of information technology, SEI based on RFF has gradually become an important research topic in the field of signal communication. This technology is of great significance in many fields, such as physical layer security authentication [1], band protection [2], malicious device authentication [3], prevention of cloning attacks, and location identification.

SEI generally includes two steps: feature extraction and classifier design. Feature extraction includes manual feature extraction and neural network based feature extraction. Classifiers are mainly divided into machine learning classifiers

The associate editor coordinating the review of this manuscript and approving it for publication was Mohammad Zia Ur Rahman .

and neural network based deep learning classifiers. The classifier training process includes supervised learning and unsupervised learning, but unsupervised learning needs to use the generation of confrontation networks or self encoders, and the recognition effect is not ideal, so the current research focuses on supervised learning. In order to solve the problem of low accuracy of individual recognition in increasingly complex electromagnetic spectrum environment, scholars have conducted extensive research on feature extraction algorithm, classifier design and recognition framework in SEI problem.

A. FEATURES EXTRACTION

Artificial feature extraction plays an important role in SEI based on machine learning. The extracted features are divided into transient features and steady-state features. When the

power amplifier switches its working state, transient characteristics will appear. The starting and ending points of transient signals, transient signal waveforms [4], power spectra [5], etc. are usually used to analyze the DNA of transient signals. The transient signal of the transmitter is not covered by the modulated signal with strong energy, and the nonlinear characteristics of the transient phase are very strong, and there are many characteristics reflecting individual differences. It is usually used to analyze burst signals [6]. In [7], a transient signal RFF recognition scheme based on logarithmic power cosine spectrum is proposed. SVM is used as a classifier to identify the extracted feature vector.

However, the transient signal has a short duration and is easily affected by environmental noise and channels, so its robustness is relatively poor. The transmitter carrier frequency offset, power amplifier nonlinearity, and quadrature modulator imbalance will lead to the generation of steady-state features. When extracting steady-state features, sample fragments need to have a long duration. The transmitter needs to extract a large amount of RF information, which can be extracted in time domain, frequency domain, and transform domain [8], such as frequency features obtained through Empirical Mode Decomposition (EMD) [9], fractal features, high-order cumulants of signals nonlinear characteristics of power amplifier, I/Q offset characteristics [10], etc.

In order to eliminate the influence of signal content difference on recognition, many researches have been done to extract the steady-state characteristics of the preamble of the signal or convert the signal characteristics into images for image recognition. In [9], the Multidimensional-Approximate-Entropy (MApEn) of the preamble structure has been extracted, and KNN classifier has been used to obtain good performance. In [11], the original sample sequence has been converted into image input. Since images are compact representations of signal information, it can ensure that the recognition accuracy is not affected by the number of input samples. Peng first proposed the concept of differential constellation diagram, and then in [12] he proposed a Radio Frequency Fingerprint (RFF) identification method based on Differential Constellation Trace Figure (DCTF) and convolutional network. The DCTF can fully represent the characteristics of I/Q imbalance, and does not need to synchronize the signal, so it has strong practicality., their method uses ZigBee as a signal generator, and DCTF is used to extract the relevant information of 2PSK signals. The recognition accuracy of 50 ZigBees can reach 99.1% and 93.8% respectively at 30 dB and 15 dB SNR levels. After that, scholars have done a lot of research on extracting steady-state features based on the differential processing of signals and constellation feature extraction methods. The differential constellation trajectories are improved by using the combination of streaming DCTFs and feature reduction algorithm to replace the single differential interval of traditional DCFT in [13], when the SNR is from 5 dB to 10 dB, the classification results of 54 ZigBee devices are 86% and 92% respectively, which is about 40% and 20% higher than the existing DCTF

based methods. In [14], a radio frequency fingerprint extraction method based on cluster center difference is proposed, which simplifies the constellation features and improves the correct recognition rate of the system under low signal-to-noise ratio, however, the calculation process of this algorithm is complex, and the results are still not optimistic. In [15], an RFF recognition method based on Hot Constellation Trace Figure (HCTF) and Slice Integrated Collaboration (SIC) is introduced, they use multiple slices to judge the final result without manually extracting features, and has strong anti-interference performance. When SNR = 0dB, the recognition accuracy can reach more than 90%, however, because too many slices are used, the training time is sacrificed to improve the recognition accuracy. In [16], ResNet was used to identify differential complex signals, and the recognition accuracy of 20 ZigBee devices reached 99% under ideal conditions.

B. NEURAL NETWORK CLASSIFIER

With the increase of the number of objects, traditional machine learning classifiers, such as random forest classifier, support vector machine classifier, have been unable to meet the requirements. In recent years, with the development of artificial intelligence and the enhancement of computing power, deep learning methods have played an important role in computer vision, speech recognition and hyperspectral data classification. The deep learning method does not need manual feature extraction, nor too much prior knowledge to complete the extraction of target features. The accuracy of deep learning identification can be improved by adjusting the network structure, optimizing the loss function [17] and optimizing the input data structure [18]. The deep learning method can identify signals in different transform domains, and can also integrate features of different transform domains. Common methods include two-dimensional time-frequency domain [19], high-order spectrum, Hilbert Huang Transform (HHT) [20], bispectrum transform, etc. The basic neural network structures include fully connected neural network, convolutional neural network, residual neural network, etc. In recent years, many researches have optimized on the basis of the classical network structure. In [21], an efficient SEI method based on Complex Valued Neural Network (CVNN) and network compression is proposed, which can reduce the complexity and size of the model under the condition of ensuring the recognition accuracy, the complexity is 10%~30% of CVNN. In [22], a new multi-channel neural network for long-term evolution terminal identification is proposed, the DCTF they use is extracted from random access preamble for synchronization, this network uses multiple downsampling transformations to automatically perform multi-scale feature extraction and classification, thus eliminating the need for manual extraction of features, experiments were carried out in Line Of Sight (LOS) and Non LOS (NLOS) scenes to classify ZigBee devices. The classification accuracy rate was 97% in LOS scenes with SNR = 30 dB or so. When the SNR was reduced, the recognition accuracy

rate could be improved by optimizing the selection of Region Of Interest (ROI) length. However, the recognition accuracy rate was seriously affected by the SNR, and only 84% was recognized when $\text{SNR} = 15$.

C. FEATURES FUSION

Previous researches on SEI mostly focused on the influence of SNR transformation on recognition results. With the complexity of electromagnetic environment, more recognition problems in different scenes need to be solved, such as NLOS conditions and Zero-Shoot conditions. Feature fusion can improve the performance of recognition in harsh environments, effective feature fusion can also give play to the advantages of each feature to improve the recognition accuracy. In [23], a closed set and open set oriented RFF recognition framework was proposed. The 14 dimensional features of the power amplifier in time domain, frequency domain, time frequency domain and fractal domain were extracted, and the extracted features were input into an improved support vector machine classifier. It was proved that feature fusion can improve the recognition accuracy under low SNR conditions, and it was found that time domain features play the most effective role in feature fusion, under ideal conditions, the recognition accuracy can reach 99% when the openness is greater than 0.074, the recognition accuracy is better than the traditional algorithm. In [24], a fusion recognition method based on (Dempster/Shافر) DS evidence theory is proposed for wireless device recognition. The recognition accuracy of the discriminator for target signals is improved by fusing the recognition results of the Nth signal segment with the recognition results of the N-1 group of signal segments. When the SNR is 5dB, the recognition accuracy can reach more than 90%, but the training process is cumbersome and the real-time performance is poor. The method in [25] fuses the features of multi domain signals, such as eye map, vector map and Hilbert VMD time spectrum, to improve the SEI accuracy. It is divided into three steps: RFF extraction, RFF generation of Artificial Radio Frequency Fingerprint (ARFF) and ARFF embedding. It makes it easier to distinguish differences between individuals by generating features, achieving a recognition accuracy of 99.91%, and the recognition rate reaches 70% when the SNR is - 2dB. It can be seen that the robustness of SEI can be improved by adding artificial features reasonably in the process of network feature extraction. In [26], the radar model identification is carried out based on the RFF extracted from the time-domain transient signal. The duration, maximum derivative, skewness, kurtosis, mean value, variance, fractal dimension, Shannon entropy, polynomial coefficient, and the area under the track curve of the normalized energy track are extracted from the radar transient signal. The extracted features are summarized into three types of RF fingerprints, and the identification accuracy of five transmitters is 91.1%, When the number of transmitters is changed, the recognition accuracy is unstable.

D. FH SIGNAL IDENTIFICATION

FH signals are generated by changing the carrier frequency according to a specific frequency hopping mode, which is usually pseudorandom. The frequency hopping spread spectrum communication mode has the advantages of excellent anti-interference performance, low interception probability, strong networking capability, etc., and is widely used in the military communication field [27]. However, due to the fast frequency hopping characteristics of FH radio stations, the fingerprint characteristics of FH radio stations are vulnerable to environmental changes. Moreover, due to the short length of each frequency hopping segment of the signal, the performance of individual steady-state characteristics is not sufficient, which makes individual identification more difficult. At present, there is little research on individual identification of FH signals. In [28], the fingerprint features of FH signals are extracted and converted into a spectrum chart representing the time-frequency behavior of signals. The spectrum chart is trained through neural networks, with an accuracy rate of 97%. However, the number of selected scenes and targets is small. Therefore, we need to verify our methods in more scenes to improve the universality of our methods.

Inspired by the traditional feature fusion methods, this paper improves the feature extraction method and feature fusion method of FH signal based on Resnet. The target selected in this paper is a PSK type frequency hopping radio station, which does not use the traditional constellation feature extraction method, but extracts the fingerprint features of the constellation after timing synchronization. This paper also improves some existing feature extraction methods, thus combining the advantages of manual feature extraction and network feature extraction to improve the accuracy of individual recognition.

Our contributions are as follows:

- 1) We extract effective constellation features, reduce the complexity on the basis of inheriting the advantages of traditional constellation features, effectively improve the recognition accuracy, and have universality for PSK signals.
- 2) We use a framework that combines deep learning and manual feature extraction. We design a suitable ResNet and input the extracted features to the full connection layer to achieve feature fusion, which proves the effectiveness and robustness of the feature fusion method.

The rest of this paper is organized as follows. The second section introduces the implementation process of the feature extraction method and our improvement on the feature extraction method. In the third section, we will introduce our feature fusion framework and simulation, and summarize in the fourth section.

II. FEATURES EXTRACTION

When there are subtle errors in the material and processing technology of the signal generation equipment, there are certain differences between the electrical parameters and nominal values of different electronic components, which is

the reason for the generation of RFF. In the transmitter, I/Q imbalance and phase noise caused by mixer, carrier frequency and phase offset caused by crystal oscillator, harmonic distortion caused by nonlinearity of digital to analog converter and nonlinear distortion of power amplifier are the main causes of RFF.

A. SIGNAL PREPROCESSING

Since the collected signal is a single channel FH signal, read the data and remove the preamble data according to the actual data segment length slice, and then intercept the data according to the effective length. After Hilbert change, the I/Q signals are obtained as:

$$\hat{X}_i(t) = H[X_i(t)] = \frac{1}{\pi} \int_{-\infty}^{\infty} \frac{X_i(\tau)}{t - \tau} d\tau \quad (1)$$

$$Y_i(t) = X_i(t) + 1j\hat{X}_i(t) \quad (2)$$

where $Y_i(t)$ is baseband complex signal, $X_i(t)$ and $\hat{X}_i(t)$ are respectively the I/Q signals, and i indicate the index of signal segments. As is shown in Fig.1, when we collect data, there are noise segments, other radio operating mode segments, etc. So we need to set the threshold value, estimate the starting point and ending point of the signal through the energy detection method. We normalize the complex data with min-max standardization.

B. CONSTELLATION GENERATION

Through the analysis, the target is 8PSK modulation mode. We think that the constellation contains the oscillation characteristics and nonlinear characteristics of the emitter, so the subtle differences of constellation can be extracted as the as fingerprint features of the signal.

Since the frequency offset and phase offset existing in the constellation have an impact, we use the octave spectrum to remove the frequency offset. mPSK signals can be represented as follows:

$$s(t) = Y(t)e^{-j\frac{2\pi m}{M}} e^{-j\omega_c t}, \quad 0 \leq t \leq T_s, \quad 0 \leq m \leq M - 1 \quad (3)$$

where T_s is the symbol period, ω_c is the signal carrier frequency, and M is the number of carrier phases that transmit information. Do nonlinear treatment for $s(t)$:

$$\begin{aligned} s^M(t) &= Y^M(t) e^{-j\frac{2\pi m}{M}M} e^{-jM\omega_c t} \\ &= Y^M(t) e^{-jM\omega_c t}, \quad 0 \leq t \leq T_s, \quad 0 \leq m \leq M - 1 \end{aligned} \quad (4)$$

At this time, there is a discrete spectral component at the M-fold carrier frequency position, which is reflected in its frequency spectrum. A discrete spectral line will appear at this position, and the carrier frequency can be estimated through the spectral line position. The specific methods are as follows:

Remove the frequency offset with the octave spectrum method, that is, use fast Fourier transform(FFT) on the octave

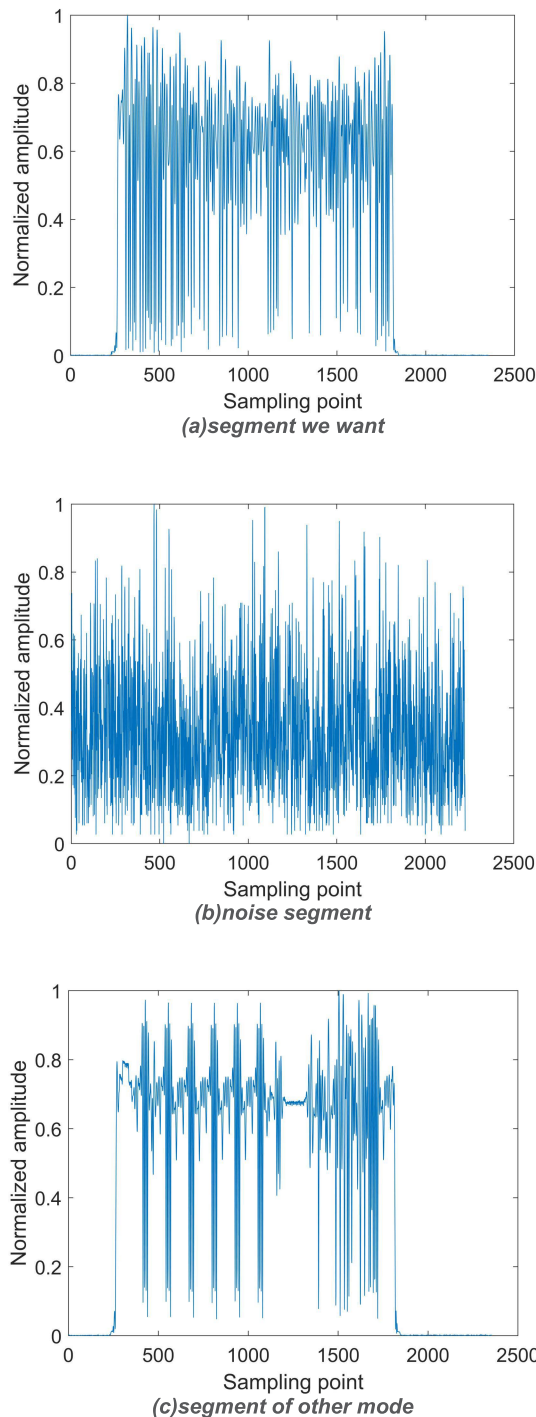


FIGURE 1. Data segments we collect.

of the complex signal $Y(t)$ to obtain its frequency offset, as shown in Fig.2.

$$f_{bias} = \text{fft}(Y^8) \quad (5)$$

$$f_0 = \frac{f_{max}f_s}{8\text{length}(Y)} \quad (6)$$

$$Y_{new} = Y e^{-2\pi j f_0 t / f_s} \quad (7)$$

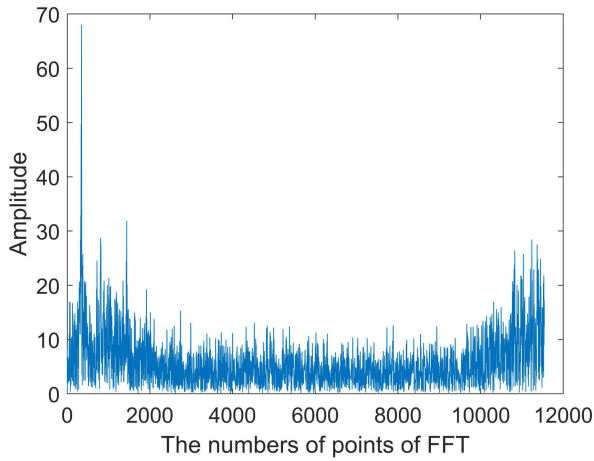


FIGURE 2. The octave spectrum.

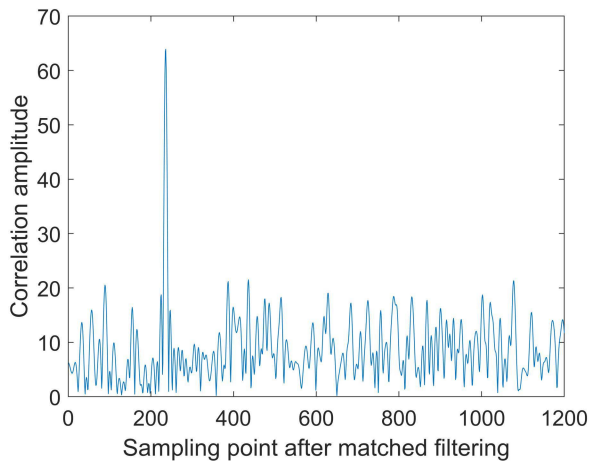
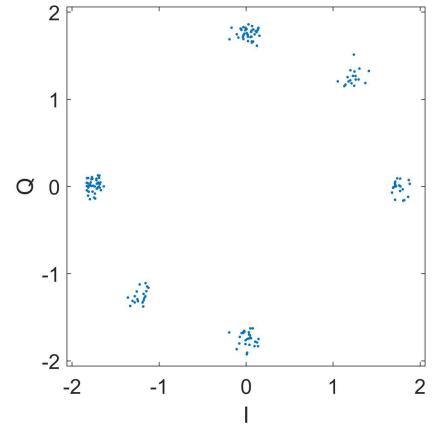


FIGURE 3. The correlation peak.

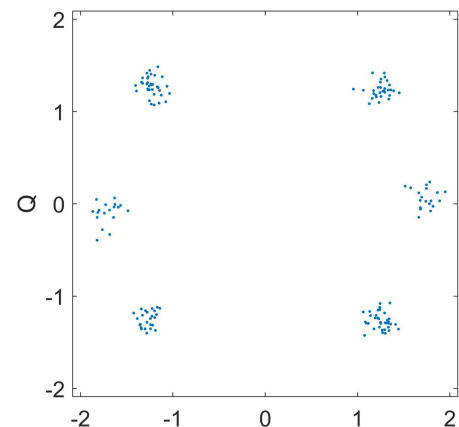
where f_{bias} is frequency offset, as shown in the figure, there is a single peak f_{max} , which is the sampling point corresponding to the maximum peak of frequency offset. Through equal scaling, f_0 is the actual frequency offset, f_s is the sampling frequency, and t is the time series. Thus, the frequency offset of each data point can be corrected.

By using 37 bit UW words we get to correlate, and using a sliding window with a length of 37 to get the correlation, the position of the correlation peak is calculated, and then the best sampling point is found. Since the sampling rate is 8 times the symbol rate, the correlation window is 8 symbols apart, and the obtained correlation peak is shown in the Fig.3. At this time, the data point corresponding to the maximum correlation peak is the best sampling point. Since the data segments have been normalized, setting the threshold of correlation peak can also filter out the interference signal segments, leaving only the data segments we are interested in.

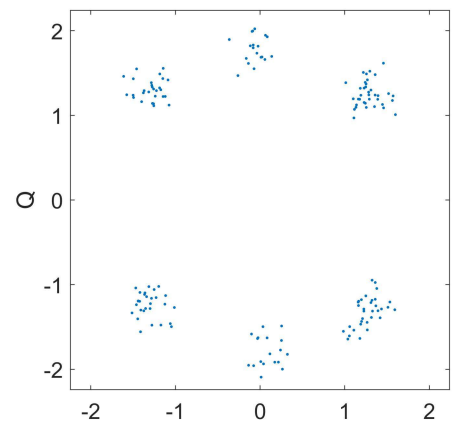
At this time, there is still phase offset in the constellation. After depolarization, the constellation is obtained as shown in the Fig.4. Because it is a mixed modulation of 2PSK and 4PSK, which is equivalent to 8PSK, there are only 6 of



(a) SNR=20dB



(b) SNR=15dB



(c) SNR=10dB

FIGURE 4. Constellation figure under different SNR.

8 phases in each frequency hopping segment, so only 6 points are displayed on the constellation.

At this time, there are differences in the direction of the constellation, so we use the improved K-means clustering algorithm to determine the direction of the constellation. Because the K-Means algorithm is very sensitive to the initial clustering center, the points of the constellation are divided

into 6 clusters through the K-Means++ algorithm, a is shown in the figure. The specific method is: assume that n data point $x_1, x_2 \dots x_n$ have been selected as the clustering center, and when selecting th $n + 1$ edata point, ensure the shortest Euclidean distance from the first n data points. The(Local Outlier Factor)LOF algorithm with outlier detection further reduces the impact of noise on constellationclustering and eliminates the impact of outliers on cluster centers by removing outliers.

Through comparison, it is found that the distance between the six cluster centers of the constellation and the origin is slightly different, and there is also a deviation from the X, Y axis and two angular bisectors of 45°, These difference can be expressed by some measure. Three kinds of constellation features are extracted: the dispersion degree of constellation, the relative distance between constellation clustering center and origin, and the deviation of constellation clustering center from the reference angle.

C. CONSTELLATION FEATURES EXTRACTION

There are six clustering centers $c_1, c_2 \dots \dots c_6$, and the points belonging to the i class ar $x_{1i}, x_{2i} \dots \dots x_{ji}$, j indicates that there are j points belonging to this class. we propose a standard to evaluate the dispersion degree μ_i , relative distance from the origin λ_i , and deviation from the reference angle of each class θ_i , expressed a:

$$\mu_i = \frac{\sum_{k=1}^j d |x_{ki} - c_i|}{j} \tag{8}$$

$$\lambda_i = \frac{d |c_i - O|}{\max(d |c_m - O|)} \quad m = 1, 2 \dots 6 \tag{9}$$

$$\theta_i = \frac{\mathbf{O}c_i \cdot \mathbf{O}A_i}{|\mathbf{O}c_i \cdot \mathbf{O}A_i|} \tag{10}$$

O is the origin, $\mathbf{O}A_i$ expressed as the corresponding reference vector of $\mathbf{O}c_i$, and relative to the reference angl θ_i is expressed as the cosine value of the included angle. Because the effect of the value $\cos \theta_i$ is too small, μ_i, λ_i is normalized, and $1 - \cos \theta_i$ is also normalized, because the quadrants of the six data points in each 8PSK data segment are different. Arrange the six data of each feature from small to large, and connect them in turn to obtain 24 feature data about each data segment. The constellation features μ_i of three FH radio set are shown in the Fig.5. Constellation angle feature $1 - \theta_i$ of three devices is shown in the Fig.6. It can be seen from the figure that there exist difference among constellation characteristics of the three devices.

D. SIMPLIFIED BOX DIMENSION FEATURES

In order to extract the difference of RFF features of different radiation source individuals, it is necessary to exclude the impact of different signal contents on the effectiveness of subtle features. Therefore, we need to select the synchroniz- ation segment of the signal, because each pulse of individu- ls of the same type and working mode has the same

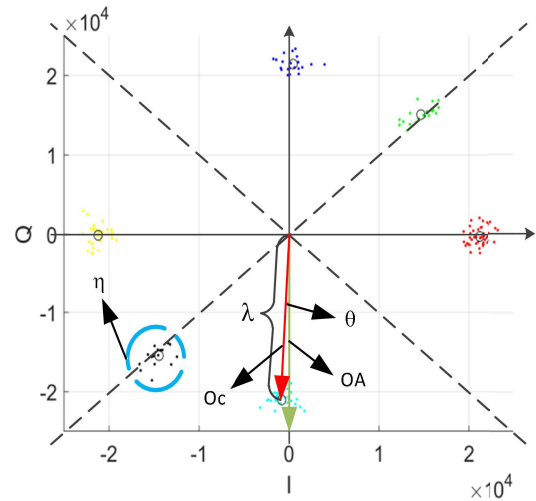


FIGURE 5. Constellation feature extraction after K-Means clustering.

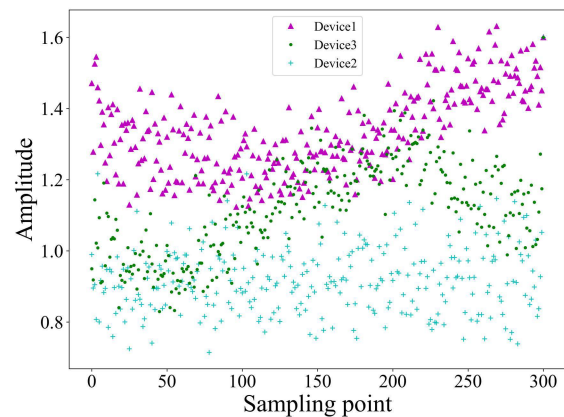


FIGURE 6. Constellation angle characteristics of three devices.

synchronzation segment. The length of the synchronization segment is 296 sampling points, and the synchronization segments of different frequency hopping radios are slightly different, as shown in Fig7. Box dimension is more intuitive in fractal analysis, and has been widely used in many research fields. So the box dimension of synchronous segment envelope can be extracted as fingerprint feature of its waveform.

Definition of box dimension: use a small box with side length ϵ_m to wrap the signal waveform, and the number of boxes required $N(\epsilon_m)$ decreases as the box length increase, as is shown in Fig.8. Take the logarithm of $N(\epsilon_m)$ and ϵ_m , draw the relation curve of $\lg N(\epsilon_m)$ and $\lg \epsilon_m$, and the slope of the curve $D_B(f)$ is the box dimension of the fractal set. The specific process is as follows:

Let f be a continuous function defined on the closed set T of the real number set R , and F be a set on R^2 :

$$F = \{(x, y) : x \in T \subset R\} \subset R^2 \tag{11}$$

If:

$$D_B(f) = \lim_{\epsilon_m \rightarrow 0} \left\{ \sup \frac{\lg N(F, \tilde{\epsilon})}{-\lg \tilde{\epsilon}} \right\} : \tilde{\epsilon} \in (0, \epsilon_m) \tag{12}$$

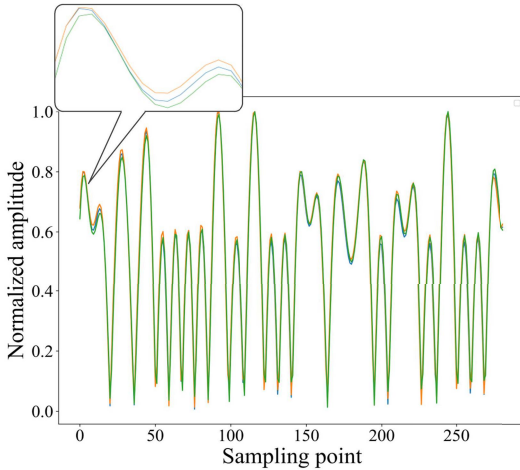


FIGURE 7. The difference of UW envelope among three devices.

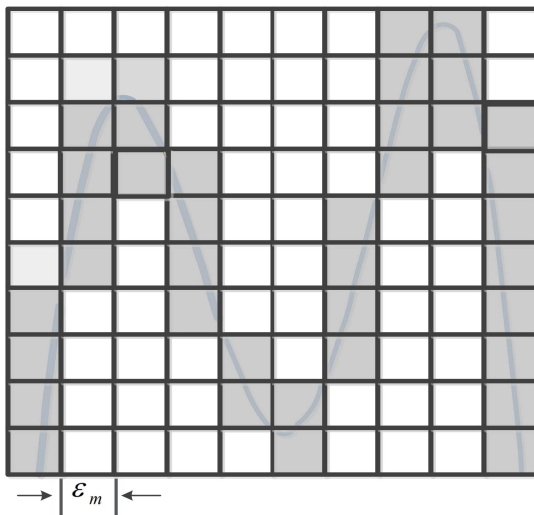


FIGURE 8. Box dimension of signal.

exists, $D_B(f)$ is the box dimension of function f , where $N(F, \tilde{\epsilon})$ is the number of boxes with size ϵ_m required to wrap the signal waveform. This process has a large amount of calculation and it is difficult to converge when the signal dimension is large, and it is found that when the box dimension is too small, the number of boxes will become unstable. In practical calculation, the fractal dimension of the set F_t of digital discrete space signal points has the following simple formula.

Set the calculated sampling sequence to $f(t_1), f(t_2), \dots, f(t_N), f(t_{N+1})$, and make:

$$d(\Delta) = \sum_{i=1}^N |f(t_i) - f(t_{i+1})| \quad (13)$$

$$d(2\Delta) = \sum_{i=1}^{N/2} \left| \max\{f(t_{2i-1}), f(t_{2i}), f(t_{2i+1})\} - \min\{f(t_{2i-1}), f(t_{2i}), f(t_{2i+1})\} \right| \quad (14)$$

$$N(\lambda) = d(\lambda)/\lambda, N(2\lambda) = d(2\lambda)/2\lambda \quad (15)$$

where $\lambda = 1/f_s$ is the sample interval, f_s is the sampling rate, then:

$$\begin{aligned} D_B(f) &= \frac{\lg \frac{N(\lambda)}{N(2\lambda)}}{\lg \frac{1/\lambda}{1/2\lambda}} \\ &= \frac{\lg N(\lambda) - \lg N(2\lambda)}{\lg 2} = 1 + \lg \frac{d(\lambda)}{d(2\lambda)} \end{aligned} \quad (16)$$

E. EXTRACTION OF OTHER FEATURES

Due to the instability of the frequency source of the radiation source equipment, the influence of internal noise and the influence of nonlinear devices, the actual signal will contain multiple frequency components. Therefore, the empirical mode decomposition (EMD) method is used to extract the spurious characteristics of the signal, and the specific methods are as follows:

After matched filtering, upconvert baseband signal to 400kHz Intermediate frequency (IF) signal, set the boundary condition ϵ , stopping decomposition when the residual component $r_n(t) < \epsilon$, and decompose the signal into n mutually orthogonal intrinsic mode function (IMF) components, as shown in the following formula, where $\text{imf}_i(t)$ is the IMF component obtained by the i -th decomposition, $\text{imf}_i(t)$ mainly contains high-frequency noise components, $r_n(t)$ is the signal trend component, and after removing these two parts, the remaining is the spurious characteristic component $s'(t)$, which is used to represent the RFF features between various components in the signal.

$$s(t) = \sum_{i=1}^n \text{imf}_i(t) + r_n(t) \quad (17)$$

$$s'(t) = \sum_{i=2}^n \text{imf}_i(t) \quad (18)$$

We use HHT to transform each component $h_i(t)$ in $s'(t)$, and then integrate the obtained signal time spectrum $H(\omega, t)$ along the time axis, that is:

$$h_i(t) = \frac{1}{\pi} \int_{-\infty}^{+\infty} \frac{\text{imf}_i(\tau)}{t - \tau} d\tau \quad (19)$$

$$H(\omega, t) = \sum h_i(t) \quad (20)$$

$$h(\omega) = \int_0^T H(\omega, t) dt \quad (21)$$

Thus, the marginal spectrum $h(\omega)$ of the signal is obtained, as is shown in Fig.9, the cumulative distribution of each frequency component in the data segment in the statistical sense is expressed by $h(\omega)$, which accurately reflects the frequency components contained in the signal. We find the frequency corresponding to the peak of $h(\omega)$, and select the first three corresponding frequencies of the largest peak as the spurious characteristics of the individual.

Skewness reflects the symmetry of the waveform, and the steepness characteristic reflects the steep fluctuation situation of the waveform and the impact characteristics of the signal. The margin factor is often used to detect the wear condition of

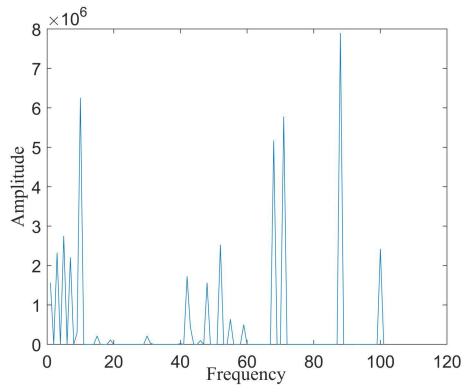


FIGURE 9. Marginal spectrum of HHT.

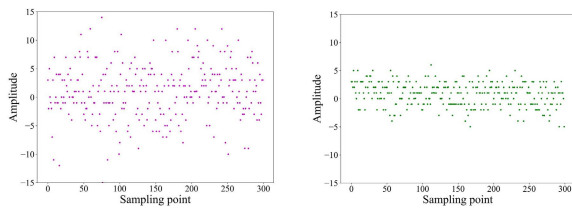


FIGURE 10. Frequency offset features of two devices.

mechanical equipment, and the waveform factor reflects the proportion of each component of the waveform as a whole.

These are the time domain characteristics of signal segments. Because we found that the frequency offset features of devices are also different, as shown in the Fig.10, we connect it with all the above features. Thus, the feature we get can be expressed as a $[1*36]$ matrix.

III. EXPERIMENTAL VERIFICATION

In this section, we collect signals of 15FH sets of the same batch, manufacturer and working mode, and their fingerprint features are obtained by using the feature extraction method introduced in the previous section. Then a neural network for individual recognition is constructed to extract the individual differences of signals. We combine the features extracted by the network with the fingerprint features we get for the final classification and recognition.

A. IMPLEMENT DETAILS

The experimental process is illustrated in Fig.11. We set the center frequency of the receiver at 230MHz and the bandwidth at 60MHz to receive FH signals from 15 FH sets in the same working mode, then we obtained baseband signal through frequency conversion, filtering and down sampling. The acquisition environment is outfield, the sampling rate is set to 1.6Mhz. Because the duration of one frequency hopping segment is about 0.94ms, so we set each sampling duration for 1.5ms, so each data segment has 2400 points. The sampling time of each radio sets lasts for 2 minutes to ensure there are enough samples. Finally, we randomly select 12000 data segments from each radio set as the data set, so the total number of data segments is $10000*15 = 180000$. Then 2000 samples are randomly selected from the segments of

each radio set as the test set, 8000 as the training set and 2000 as the verification set to find the best model parameters.

We set epoch = 20, batchsize = 1024, learning rate = 0.001, and we use the exponential decay learning rate to optimize the convergence effect of training. We choose the Cross-EntropyLoss as the loss function and Adam as optimizer. We use label smoothing method with epsilon = 0.1, and we add BatchNormalization(BN) layers to prevent over fitting.

Take the absolute value of the signal and input it into the neural network. At the same time, input the constellation features and other features extracted from the data segment into the full connection layer, so as to complete the fusion of our extracted features and network extracted features.

B. EXPERIMENTAL RESULTS AND ANALYSE

In order to verify the effectiveness, robustness and universality of the method proposed in this paper, and select the appropriate network structure to improve the recognition accuracy, three comparative experiments are carried out.

First, we compared the impact of different network structures on the recognition accuracy. Using the methods presented in this article, by comparing the influence of four classical network structures on the recognition accuracy of 15 FH radios under different SNR conditions, we design a network structure suitable for the methods in this paper.

From Figure 12, we can see that the recognition accuracy of ResNet18 can reach 95.03% when the SNR is 30dB, and it still has 77.62% when the SNR ratio is 10dB. As a comparison, the recognition accuracy of VGG16 is 91.14% when the SNR is 30dB, which shows that the ResNet can improve the recognition accuracy and performs well under low SNR conditions. The structure of GoogLeNet is complex, the training time is long, and the over fitting is serious, which is not suitable for the signal individual recognition method proposed in this paper. The structure of ResNet we designed is presented in Table 1, the network structure consists of three residual blocks, two convolution layers and two fully connected layers, a fully connected layer is added to make the network output adjust to the same order of magnitude as the feature array we extract, so that the features we extract can play a role in the testing process.

It can be seen from the Fig12 that our network inherits the good anti noise performance of Resnet, it has a simpler structure than ResNet18, and has higher recognition accuracy.

The confusion matrixes at 15 dB and 30 dB SNRs for the 15 FH radio sets devices identification are depicted in Fig.13. It can be seen from the picture that device 3 and device 4 have higher misclassification rate, indicating that some radio stations have similar RFF features.

Since this paper uses the constellation features, in order to verify the universality of this method, we simulated 15 individuals of BPSK, QPSK and 16QAM modulation signals. Since the mixed modulation method of 2PSK and 4PSK used in this paper is equivalent to 8PSK modulation signal, we calculate it as 8PSK signal for comparison. Figure 10 shows

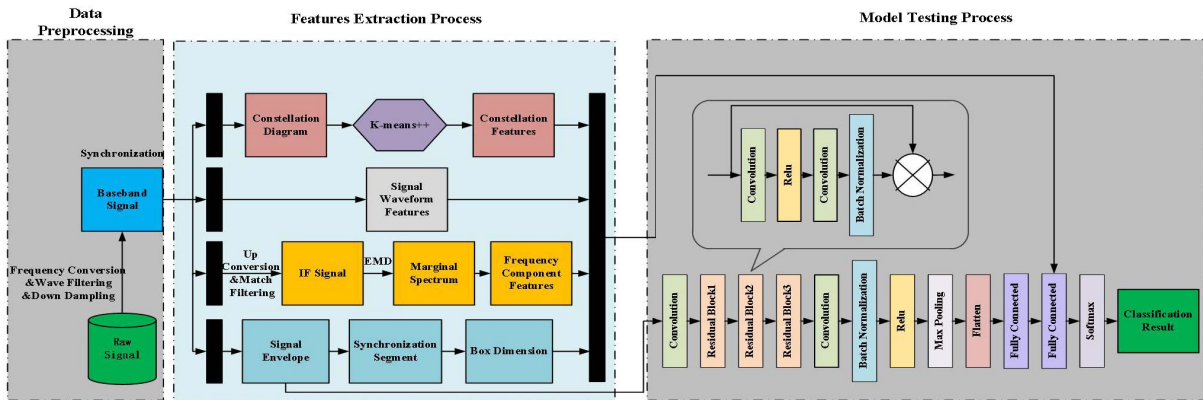


FIGURE 11. Experimental process.

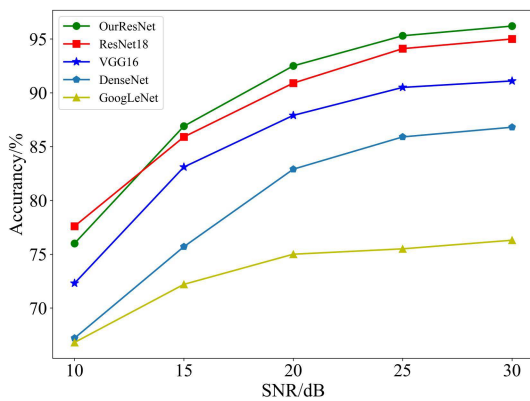


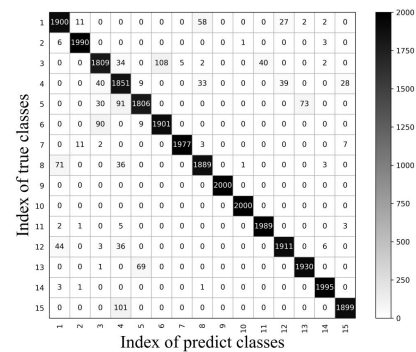
FIGURE 12. Recognition accuracy under different network structures and different SNR.

TABLE 1. The structure of our ResNet.

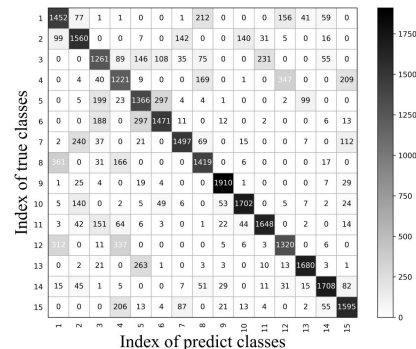
Number	Layers	Output shape
1	Input	1×1500
2	Conv1	4×750
3	Res Block1	16×750
4	Res Block2	64×375
5	Res Block3	128×188
6	Conv2	256×94
7	Avg Pooling	256×1
8	Flatten	256
9	FC	64
10	FC/Softmax	15

the recognition accuracy of different modulation methods in AWGN channel, and the SNR is 10-30dB.

As we can see from Fig 14, In the contrast experiment of recognition of simulated signals with different modulation modes, several types of signals can achieve high individual recognition accuracy, which proves the effectiveness of the method in this paper. The recognition accuracy of signals



(a) SNR=30



(b) SNR=15

FIGURE 13. Confusion matrixes at 30 dB and 15 dB for the 15 FH devices identification.

decreases significantly when the SNR is below 22dB. BPSK belongs to signals with less frequency components, and have high recognition accuracy under different SNR. Even if the SNR is 10dB, it has an accuracy of 92.59%. When the SNR is 30dB, it has an accuracy of 98.12%. The 4QAM modulation mode is vulnerable to noise. When the SNR is more than 22dB, the recognition accuracy can reach more than 95%. When the SNR is less than 16dB, the recognition accuracy is lower than 8PSK and 16QAM, 16QAM belongs to amplitude phase joint modulation signal, which contains a lot of amplitude information and performs well under low SNR conditions.

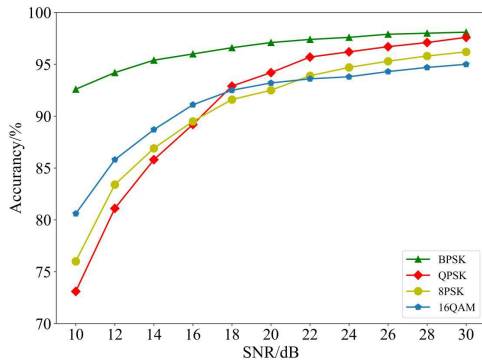


FIGURE 14. Recognition accuracy under different modulation modes and different SNR.

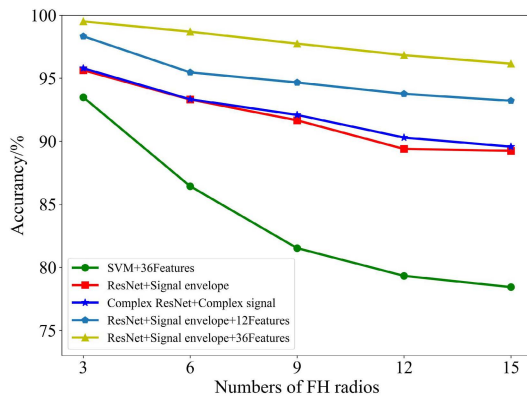


FIGURE 15. The recognition accuracy of different algorithms and different numbers of individuals under the SNR of 30dB.

In the third experiment, we set the SNR to 30dB, we compare the method proposed in this paper with the other four methods to prove the effectiveness of the feature fusion method and the effectiveness of constellation features. By studying the individual recognition accuracy under different individual quantity conditions, we prove the adaptability of the method in this paper under the scenario of terminal quantity change:

1. Use random forest classifier to classify $[1 * 36]$ fingerprint features extracted in this paper.

2. Use residual neural network to extract features of signal envelope.

3. Use complex neural network to extract features of complex signal.

4. Remove the constellation features, use the remaining $[1 * 12]$ fingerprint features and signal envelope, and use the method proposed in this paper to detect the accuracy of individual recognition.

5. Method in this paper.

Fig. 15 demonstrates that when the number of individuals is small, each method has a high recognition accuracy. With the increase of the number of individuals, the recognition accuracy of various algorithms decreases. In the case of three individuals, the recognition accuracy of the method in this paper can reach 99.52%. The method based on feature extraction has a low recognition accuracy when the number of individuals is large. The method of complex signal recognition using

complex residual network and the method of signal envelope recognition using ResNet have similar recognition accuracy. Compared with the residual network method for extracting signal envelope features, the method in this paper adds the features we extract to improve the recognition accuracy. Different from method 4, the method proposed in this paper adds more constellation features. Compared with the recognition accuracy of 93.21% in method 4, the constellation features improve the recognition accuracy by nearly 3%, the effectiveness of the proposed constellation features is proved.

IV. CONCLUSION AND FUTURE WORK

In this paper, we obtain constellation with clear clustering, propose a constellation feature extraction method, use an extraction method based on constellation feature, frequency offset feature, HHT marginal spectrum feature, simplified box dimension feature and waveform features, and we design appropriate residual network structure to improve the recognition accuracy. The main conclusions are as follows:

1) Compared with the traditional individual recognition method based on neural network, the recognition method of data and feature fusion used in this paper makes the recognition accuracy of 15 FH radios reach 96.16% at 30dB SNR. The addition of RFF improves the recognition accuracy, and the constellation features extracted in this paper improve the recognition accuracy by 3%.

2) Constellation features are applicable to all kinds of PSK signal recognition problems, and the recognition performance of BPSK and 16QAM modulation signals is good.

3) Compared with other network structures, the residual network has higher recognition accuracy under various SNR conditions and is relatively simple in structure.

4) In the problem of individual recognition, when the number of individuals increases, the deep learning method is more effective than the traditional method of machine learning.

Because the acquisition of constellation features requires synchronization and the process is cumbersome, we plan to study the feature extraction of *DCFT* in the next step to simplify the feature acquisition process. We also want to apply our method to *Differential Complex-Valued Neural Network* to observe the recognition results.

REFERENCES

- [1] C. Hou, G. Liu, Q. Tian, Z. Zhou, L. Hua, and Y. Lin, "Multisignal modulation classification using sliding window detection and complex convolutional network in frequency domain," *IEEE Internet Things J.*, vol. 9, no. 19, pp. 19438–19449, Oct. 2022.
- [2] L. Sun, X. Wang, Z. Huang, and B. Li, "Radio-frequency fingerprint extraction based on feature inhomogeneity," *IEEE Internet Things J.*, vol. 9, no. 18, pp. 17292–17308, Sep. 2022.
- [3] Z. Bao, Y. Lin, S. Zhang, Z. Li, and S. Mao, "Threat of adversarial attacks on DL-based IoT device identification," *IEEE Internet Things J.*, vol. 9, no. 11, pp. 9012–9024, Jun. 2022.
- [4] G. Shen, J. Zhang, A. Marshall, and J. R. Cavallaro, "Towards scalable and channel-robust radio frequency fingerprint identification for LoRa," *IEEE Trans. Inf. Forensics Security*, vol. 17, pp. 774–787, 2022.
- [5] J. Yang, Z. Qin, Q. Zhang, and T. Yang, "Research on modulation mode identification of PSK signal based on M-th power spectrum features," in *Proc. 10th Int. Conf. Intell. Comput. Wireless Opt. Commun. (ICWOC)*, Jun. 2022, pp. 25–28.

- [6] K. Wang, Z. Dong, T. Wan, K. Jiang, W. Xiong, and X. Fang, "Research on radar active deception jamming identification method based on RESNET and bispectrum features," in *Proc. Int. Conf. Comput. Eng. Appl. (ICCEA)*, Jun. 2021, pp. 491–495.
- [7] J. Zhang, Q. Wang, X. Guo, X. Zheng, and D. Liu, "Radio frequency fingerprint identification based on logarithmic power cosine spectrum," *IEEE Access*, vol. 10, pp. 79165–79179, 2022.
- [8] Y. Wang, G. Gui, H. Gacanin, T. Ohtsuki, O. A. Dobre, and H. V. Poor, "An efficient specific emitter identification method based on complex-valued neural networks and network compression," *IEEE J. Sel. Areas Commun.*, vol. 39, no. 8, pp. 2305–2317, Aug. 2021.
- [9] L. Sun, X. Wang, A. Yang, and Z. Huang, "Radio frequency fingerprint extraction based on multi-dimension approximate entropy," *IEEE Signal Process. Lett.*, vol. 27, pp. 471–475, 2020.
- [10] L. Ying, J. Li, and B. Zhang, "Differential complex-valued convolutional neural network-based individual recognition of communication radiation sources," *IEEE Access*, vol. 9, pp. 132533–132540, 2021.
- [11] L. Ding, S. Wang, F. Wang, and W. Zhang, "Specific emitter identification via convolutional neural networks," *IEEE Commun. Lett.*, vol. 22, no. 12, pp. 2591–2594, Dec. 2018.
- [12] L. Peng, J. Zhang, M. Liu, and A. Hu, "Deep learning based RF fingerprint identification using differential constellation trace figure," *IEEE Trans. Veh. Technol.*, vol. 69, no. 1, pp. 1091–1095, Jan. 2020.
- [13] Y. Li, Y. Ding, J. Zhang, G. Goussetis, and S. K. Podilchak, "Radio frequency fingerprinting exploiting non-linear memory effect," *IEEE Trans. Cognit. Commun. Netw.*, early access, Oct. 6, 2022, doi: 10.1109/TCNN.2022.3212414.
- [14] M. Li, "Electronic radar signal recognition based on wavelet transform and convolutional neural network," in *Proc. 2nd Asia-Pacific Conf. Commun. Technol. Comput. Sci. (ACCTCS)*, Feb. 2022, pp. 470–474.
- [15] Y. Peng, P. Liu, and Y. Wang, "Radio frequency fingerprint identification based on slice integration cooperation and heat constellation trace figure," *IEEE Wireless Commun. Lett.*, vol. 11, no. 3, pp. 543–547, Mar. 2022.
- [16] K. Merchant, S. Revay, G. Stantchev, and B. Nousain, "Deep learning for RF device fingerprinting in cognitive communication networks," *IEEE J. Sel. Topics Signal Process.*, vol. 12, no. 1, pp. 160–167, Feb. 2018.
- [17] J. Wang, B. Zhang, J. Zhang, N. Yang, G. Wei, and D. Guo, "Specific emitter identification based on deep adversarial domain adaptation," in *Proc. 4th Int. Conf. Inf. Commun. Signal Process. (ICICSP)*, Sep. 2021, pp. 104–109.
- [18] V. R. M. Elias, V. C. Gogineni, W. A. Martins, and S. Werner, "Kernel regression over graphs using random Fourier features," *IEEE Trans. Signal Process.*, vol. 70, pp. 936–949, 2022.
- [19] X. Wu, J. Zhang, C. Hou, G. Liu, J. Zhang, and J. Liu, "Signal modulation recognition based on convolutional autoencoder and time-frequency analysis," in *Proc. 8th Int. Conf. Dependable Syst. Their Appl. (DSA)*, Aug. 2021, pp. 664–668.
- [20] J. Li, Z. Liang, Y. Qi, L. Li, G. Li, N. Zheng, and Z. Wang, "Feature extraction and state identification of transformer DC bias vibration based on HHT-SVM," in *Proc. 7th Asia Conf. Power Electr. Eng. (ACPEE)*, Apr. 2022, pp. 746–750.
- [21] T. Wang, H. Liu, and J. Li, "Spectral-spatial classification of few shot hyperspectral image with deep 3-D convolutional random Fourier features network," *IEEE Trans. Geosci. Remote Sens.*, vol. 60, pp. 1–18, 2022.
- [22] P. Yin, L. Peng, J. Zhang, M. Liu, H. Fu, and A. Hu, "LTE device identification based on RF fingerprint with multi-channel convolutional neural network," in *Proc. IEEE Global Commun. Conf. (GLOBECOM)*, Dec. 2021, pp. 1–6.
- [23] T. Yang, J. Zhao, X. Wang, and F. Xu, "Deep learning based RFF recognition with differential constellation trace figure towards closed and open set," in *Proc. IEEE/CIC Int. Conf. Commun. China (ICCC)*, Aug. 2022, pp. 2377–8644.
- [24] B. Li and E. Cetin, "Design and evaluation of a graphical deep learning approach for RF fingerprinting," *IEEE Sensors J.*, vol. 21, no. 17, pp. 19462–19468, Sep. 2021.
- [25] Z. Zhang, A. Hu, W. Xu, J. Yu, and Y. Yang, "An artificial radio frequency fingerprint embedding scheme for device identification," *IEEE Commun. Lett.*, vol. 26, no. 5, pp. 974–978, May 2022.
- [26] S. Guo, S. Akhtar, and A. Mella, "A method for radar model identification using time-domain transient signals," *IEEE Trans. Aerosp. Electron. Syst.*, vol. 57, no. 5, pp. 3132–3149, Oct. 2021.
- [27] S. Liu, Y. D. Zhang, T. Shan, and R. Tao, "Structure-aware Bayesian compressive sensing for frequency-hopping spectrum estimation with missing observations," *IEEE Trans. Signal Process.*, vol. 66, no. 8, pp. 2153–2166, Apr. 2018.
- [28] J. Kang, Y. Shin, H. Lee, J. Park, and H. Lee, "Radio frequency fingerprinting for frequency hopping emitter identification," *Appl. Sci.*, vol. 11, no. 22, p. 10812, Nov. 2021.



MINGDI LI was born in Shijiazhuang, China, in 1998. He received the B.S. degree in automation from the Huazhong University of Science and Technology, in 2020. He is currently pursuing the M.S. degree with The 54th Research Institute of CETC.

He joined the Summer Workshop of NUS, in 2018, and studied in the National Defense University of Science and Technology as an Exchanged Student, in China, in 2021. His current research interests include signal processing and artificial intelligence.



JUN XIE received the B.S. degree from the University of Electronic Science and Technology and the M.S. degree from Xidian University. He is currently a Professor (Status High Level Engineer) with The 54th Research Institute of CETC. His research interest includes area of communication countermeasure.



HONGJIE YANG received the B.S. degree from the Nanjing University of Technology, in 2016, and the M.S. degree from The 54th Research Institute of CETC, in 2019. He is currently an Assistant Engineer with The 54th Research Institute of CETC. His research interest includes area of artificial intelligence.



MENGJIE GENG received the B.S. degree from Xidian University, in 2017, and the M.S. degree from The 54th Research Institute of CETC, in 2020. She is currently an Assistant Engineer with The 54th Research Institute of CETC. Her research interests include area of signal processing and artificial intelligence.



JICHUAN LIU (Member, IEEE) received the B.S. and M.S. degrees from Yanshan University and the Ph.D. degree from Xidian University. He is currently a Senior Engineer with The 54th Research Institute of CETC. His research interests include area of electronic countermeasures and cluster intelligence.